Published in final edited form as:
J Comp Neurol. 2009 July 20; 515(3): 313–330. doi:10.1002/cne.22017.

Efferent projections of thyrotropin-releasing hormone-synthesizing neurons residing in the anterior parvocellular subdivision of the hypothalamic paraventricular nucleus

Gábor Wittmann[1], **Tamás Füzesi**[1], **Praful S. Singru**[2], **Zsolt Liposits**[1,3], **Ronald M. Lechan**[2,4], and **Csaba Fekete**[1,2]

[1]Department of Endocrine Neurobiology, Institute of Experimental Medicine, Hungarian Academy of Sciences, Budapest, Hungary

[2]Tupper Research Institute and Department of Medicine, Division of Endocrinology, Diabetes, and Metabolism, Tufts Medical Center, 800 Washington St, Boston, MA, 02111

[3]Department of Neuroscience, Faculty of Information Technology, Pázmány Péter Catholic University, Budapest, Hungary

[4]Department of Neuroscience, Tufts University School of Medicine, Boston, Massachusetts 02111

Abstract

The anterior parvocellular subdivision of the PVN (aPVN) contains non-hypophysiotropic TRH neurons that are densely innervated by feeding-related neuronal groups of the hypothalamic arcuate nucleus. To determine how these TRH neurons are integrated within the brain, the major projection fields of this cell group was studied by anterograde and retrograde tract-tracing methods. Projection sites were identified by injection of the anterograde tracer *Phaseolus vulgaris* leuco-agglutinin (PHAL) into the aPVN, and subsequent double immunofluorescent staining was used to visualize axons containing both PHAL and proTRH. To distinguish between the projection sites of TRH neurons residing in the aPVN and the closely situated perifornical area. the retrograde tracer, cholera toxin B subunit (CTB), was injected into regions where PHAL/proTRH-containing axons were densely accumulated. TRH neurons in the aPVN were found to project to the hypothalamic arcuate, dorsomedial and ventral premammillary nuclei, medial preoptic region, tuber cinereum area, paraventricular thalamic nucleus, bed nucleus of the stria terminalis, lateral septal nucleus and central amygdaloid nucleus. Projection fields of perifornical TRH neurons were in partial overlap with that of the aPVN TRH cells. In addition, these neurons also innervated the hypothalamic ventromedial nucleus, the medial amygdaloid nucleus and the amygdalo-hippocampal area. These data suggest that through its efferent connections, aPVN TRH neurons may be involved in the regulation of energy homeostasis co-ordinately with effects on behavior, locomotor activity and thermogenesis. In addition, the major differences in the projection fields of aPVN and perifornical TRH neurons suggest that these two TRH-synthesizing neuronal groups are functionally different.

Keywords

TRH; paraventricular nucleus; perifornical; anterograde; retrograde

Corresponding Author: Csaba Fekete M.D., Ph. D. Department of Endocrine Neurobiology Institute of Experimental Medicine Hungarian Academy of Sciences 43 Szigony St Budapest, Hungary 1083 Phone: 36-1-210-9947 Fax: 36-1-210-9961 E-mail: feketecs@koki.hu .

Introduction

Thyrotropin-releasing hormone (TRH), an amidated, three amino acid peptide, is widely expressed in the brain and acts as neurotransmitter (Lechan and Segerson, 1989). In accordance with its widespread distribution, TRH is involved in a number of CNS functions such as neuroendocrine regulation, arousal, thermoregulation, analgesia and autonomic control (Lechan, 1993). The best studied and characterized population of TRH producing neurons are the hypophysiotropic TRH neurons that control the hypothalamic-pituitary-thyroid axis. Their cell bodies are located in the medial and periventricular parvocellular subdivisions of the hypothalamic paraventricular nucleus (PVN) (Ishikawa et al., 1988; Kawano et al., 1991; Merchenthaler and Liposits, 1994), and their axons project to the median eminence where TRH is secreted into the portal capillaries for conveyance to thyrotroph cells of the anterior pituitary. Much less is known, however, about the roles of other distinct, topographically well-defined populations of TRH neurons of the brain.

In addition to the hypophysiotropic TRH neurons, the PVN also contains a prominent group of TRH neurons located in the anterior parvocellular subdivision (aPVN) of this nucleus. Since TRH neurons in the aPVN do not project to the median eminence (Ishikawa et al., 1988; Kawano et al., 1991; Merchenthaler and Liposits, 1994), these neurons do not subserve a hypophysiotropic function. In addition, contrary to hypophysiotropic TRH neurons, proTRH gene expression in the aPVN is not regulated by negative feedback of circulating levels of thyroid hormones (Nishiyama et al., 1985; Segerson et al., 1987b) and they do not synthesize the peptide, cocaine- and amphetamine-regulated transcript (CART) (Fekete et al., 2000b). Nevertheless, similar to medial and periventricular TRH neurons, aPVN TRH cells are heavily innervated by axons containing agouti-related protein (AGRP)/neuropeptide Y (NPY) and α-melanocyte-stimulating hormone (α-MSH)/CART (Fekete et al., 2000a; Legradi and Lechan, 1999), originating in two separate neuronal populations of the arcuate nucleus that are well-known as principal regulators of food intake and energy expenditure (Schwartz et al., 2000). These data raise the possibility that like hypophysiotrophic TRH neurons in the medial and periventricular subdivisions of the PVN, aPVN TRH neurons may also contribute to the neuronal network involved in the control of energy homeostasis.

As a first step in the elucidation of the functions of aPVN TRH neurons, we mapped the major projection sites of these neurons. For this purpose, we injected the anterograde neuronal tracer *Phaseolus vulgaris* leuco-agglutinin into the aPVN and examined the distribution of anterogradely labeled TRH-containing axons in the brain. Since another group of non-hypophysiotropic TRH neurons, the rostro-laterally located perifornical TRH cell population, are adjacent to the aPVN (Lechan and Jackson, 1982; Segerson et al., 1987a), we also performed retrograde tract-tracing experiments to separate the projection sites of the TRH neurons in the aPVN and in the perifornical region.

Materials and Methods

2.1. Animals

Adult male Wistar (TOXI-COOP KKT, Budapest, Hungary) and Sprague—Dawley rats (Taconic Farms, Germantown, NY), weighing 260–400 g were used throughout this study. Animals were housed under standard conditions (lights on between 06.00 and 18.00 h, temperature 22±1 °C, rat chow and water *ad libitum*). All experimental protocols were reviewed and approved by the Animal Welfare Committees at the Institute of Experimental Medicine of the Hungarian Academy of Sciences and Tufts Medical Center.

2.2. Anterograde tract-tracing experiments

The anterograde tracer *Phaseolus vulgaris* leuco-agglutinin (PHAL; Vector Laboratories, Burlingame, CA) was injected by iontophoresis into the region of aPVN of 17 animals. Rats were anesthetized i.p. with ketamine-xylazine (ketamine: 50 mg/kg; xylazine: 10 mg/kg body weight) and their head positioned in a stereotaxic apparatus with the bregma and lambda in the horizontal plane. Through a burr hole in the skull, a glass micropipette (20 μm outer tip diameter) filled with 2.5% PHAL in 0.01M phosphate buffer (PB) at pH 8.0 was lowered into the brain at stereotaxic coordinates corresponding to the aPVN, based on the atlas of Paxinos and Watson (Paxinos and Watson, 1998). The tracer was deposited by iontophoresis for 11-15 min (6 μA positive current, pulsed on—off at 7 s intervals) using a constant-current source (Stoelting, Wood Dale, IL). Rats were allowed to survive for 9-14 days, then deeply anesthetized with ketamine-xylazine and were perfused transcardially with 20 ml 0.01M phosphate buffered saline (PBS; pH 7.4), followed by 150 ml of 4% paraformaldehyde in 0.1M PB, pH 7.4. The brains were rapidly removed, cut into two blocks and cryoprotected by immersion in 30% sucrose in PBS overnight. The forebrains and brainstems were sectioned at 25 μm with a freezing microtome (Leica Microsystems, Wetzlar, Germany). Series of sections, obtained at 100 μm intervals, were collected into antifreeze solution (30% ethylene glycol; 25% glycerol; 0.05M PB) and stored at -20°C until their use for for immunohistochemistry.

Single-labeling PHAL immunohistochemistry was performed to evaluate the injection sites. Sections were pre-treated with 0.5% H_2O_2 and 0.5% Triton X-100 in PBS for 15 min. Non-specific antibody binding was reduced by treatment in 2% normal horse serum in PBS. Sections were incubated in rabbit anti-PHAL antiserum (Vector) at 1:5000, diluted in PBS containing 2% normal horse serum and 0.2% sodium azide (antibody diluent) for 1 day at room temperature. After washing in PBS, sections were incubated in biotinylated donkey anti-rabbit IgG (Jackson ImmunoResearch, West Grove, PA) at 1:500 for 2 h at room temperature. After further rinsing in PBS, the sections were incubated in avidin-biotin-peroxidase complex (ABC Elite Kit, Vector) at 1:1000 dilution for 1 h. Following rinses in PBS, the tissue-bound peroxidase activity was visualized by 0.05% diaminobenzidine and 0.15% nickel ammonium sulfate with 0.005% H_2O_2 in 0.05 M Tris buffer at pH 7.6. The sections were counterstained with 1% cresyl violet, mounted onto glass slides and coverslipped with Depex mounting medium.

Sections from 4 animals with injection sites in the aPVN/perifornical area were used for double immunofluorescence to identify the axons that contain both PHAL- and proTRH-immunoreactivity. Following standard pre-treatment as described above for single labeling, sections were incubated in a mixture of primary antisera: goat anti-PHAL (Vector) at 1:1000 and rabbit anti-proTRH 178-199 peptide, diluted at 1:2500 (gift from Dr. Éva Rédei, Northwestern University, Chicago, IL) for 2 days at 4°C. After washes in PBS, sections were immersed in a cocktail of biotinylated donkey anti-sheep at 1:500 (Jackson) and CY3-conjugated donkey anti-rabbit IgG (Jackson, 1:200) and incubated for 2 h at room temperature. After rinsing with PBS, sections were transferred into ABC at 1:1000 for 2 h. The sections were rinsed in PBS and then amplified with biotinylated tyramide using the TSA amplification kit (Perkin Elmer Life and Analytical Sciences, Waltham, MA). After further washes, the sections were incubated in Fluorescein DTAF-conjugated Streptavidin (1:300, Vector) for 2 h and mounted onto glass slides. To facilitate identification of brain nuclei, sections were coverslipped with Vectashield Mounting Medium with DAPI (Vector).

2.3. Retrograde tract-tracing experiments

The retrograde tracer, cholera toxin β subunit (CTB, List Biological Laboratories, Campbell, CA) was injected into specific brain regions where the majority PHAL/proTRH containing,

double labelled axons were found in the anterograde tract-tracing experiment. Animals were anesthetized i.p. with ketamine-xylazine and their heads mounted in a stereotaxic apparatus as described above. At stereotaxic coordinates corresponding to each target region, a glass micropipette with 20 μm outer tip diameter, filled with 0.5% CTB was lowered into the brain through a burr hole. CTB was iontophoresed by a 6 μA positive current, pulsed on—off at 7 s intervals over 10-15 min for each injection. Following a 6–10 day transport time, animals were re-anesthetized and stereotaxically injected with 60 μg colchicine into the lateral cerebral ventricle to enhance the immunocytochemical detection of TRH in cell bodies. After 20 h survival, the animals were deeply anesthetized with ketamine-xylazine and perfused first with 20 ml PBS, followed sequentially by 100 ml of 3% paraformaldehyde/1% acrolein in 0.1M PB and 50 ml of 3% paraformaldehyde in the same buffer. The brains were removed, immersed in 30% sucrose for 1–2 days, frozen on dry ice and 25-μm-thick coronal sections were cut on a freezing microtome into one-in-four series of sections.

The location of CTB injection sites and the distribution of CTB-containing TRH neurons in the aPVN and perifornical area were studied in double-immunolabeled sections. One of the four series of sections was pre-treated sequentially first with 1% sodium borohydride in distilled water for 30 min, followed by 0.5% H_2O_2 and 0.5% Triton X-100 in PBS for 15 min, and then 2% normal horse serum in PBS for 20 min. Sections were then incubated in the mixture of goat anti-CTB antiserum (List Biological Labs) at 1:10000 and rabbit anti-TRH antiserum (no. 31, a gift from Dr. Ivor M. Jackson, Brown Medical School, Providence, RI) at 1:2500 for 2 days at 4°C. Following washes in PBS, the sections were immersed in a mixture of biotinylated donkey anti-sheep at 1:500 (Jackson) and CY3-conjugated donkey anti-rabbit IgG (Jackson, 1:200), and incubated for 2 h at room temperature. After rinsing with PBS, sections were incubated in ABC at 1:1000 for 2 h. The sections were rinsed in PBS and subjected to biotinylated tyramide amplification as above for 15 min. After further washes, the sections were incubated in Fluorescein DTAF-conjugated Streptavidin (1:300, Vector) for 2 h, mounted onto glass slides and coverslipped with Vectashield (Vector).

2.4. Image and data analysis

Double fluorescent preparations were examined with a Zeiss AxioImager M1 epifluorescent microscope (Carl Zeiss AG, Göttingen, Germany). To facilitate identification of double-labeled axons and cell bodies, sections were examined under fluorescent illumination through Zeiss Filter Set 23: excitation 475-495 and 540-552 nm, beam splitter 500 and 560 nm, emission 515-530 and 580-630 nm. For unequivocal detection of the signals of individual fluorochromes and for taking images the following filter sets were used: for Fluorescein DTAF excitation filter of 450–490 nm, beam splitter of 495 nm, and emission filter of 500–550 nm; for CY3, excitation of 538–562 nm, beam splitter of 570 nm, and emission filter of 570–640 nm. Images were captured either with the Zeiss AxioImager M1 microscope using AxioCam MRc 5 digital camera (Zeiss) and AxioVision 4.6 software (Zeiss), or with a Radiance 2100 confocal microscope (Bio-Rad Laboratories, Hemel Hempstead, UK). Confocal images were taken using line by line sequential scanning with laser excitation lines 488 nm for Fluorescein DTAF and 543 nm for CY3 555; beamsplitter/emission filters, 560/500–530 nm for Fluorescein DTAF, and 560–625 nm for CY3. For 20x and 40x oil lenses, pinhole sizes were set to obtain optical slices of 2 and 1 μm thickness, respectively, and the series of optical sections were recorded with 2.0 and 1.0 μm Z step. To enhance visibility of double-labeled PHAL/proTRH and CTB/TRH cell bodies, consecutive optical sections (from 3 to 12) were projected into one image with ImageJ image analysis software (public domain at http://rsb.info.nih.gov/ij/download/src/). Brightfield images of the PHAL injection sites were captured with Zeiss AxioImager M1 microscope. Adobe

Photoshop 7.0 (Adobe Systems Incorporated, San Jose, CA) and an IBM compatible personal computer was used to create composite images and to modify brightness and contrast of the images.

PHAL/proTRH-containing axon terminals and en-passant boutons were considered in the analysis as projections of aPVN or perifornical TRH neurons. Line drawings representing the distribution of double-labeled PHAL/proTRH-IR fibers and CTB/TRH-IR neurons were made using Corel Draw 11 (Corel Corporation, Ottawa, Canada). Cell counts of CTB/TRH-IR neurons in the aPVN and perifornical area were counted in 1 in 4 series of 25 μm thick sections from each brain with successful CTB injections. In sections of the CTB-injected brains, the aPVN and the perifornical area were identified by the distribution, shape and orientation of the TRH-IR neurons (Fig. 1).

2.5. Antibody characterization

Please see Table 1 for a list of primary antibodies used.

According to descriptions of the manufacturers, the PHAL antiserum was produced by hyperimmunization of goat with purified PHAL and specific antibodies to PHAL were isolated by affinity chromatography on PHAL-agarose columns, whereas the CTB antiserum forms an immunoprecipitin band against a 0.5 mg/ml solution of cholera toxin B subunit. Since PHAL and CTB are normally not present in the brain, the specificity of PHAL and CTB antisera were verified by the lack of any labeling in brain sections from animals that were not injected with PHAL and CTB.

The specificity of rabbit anti-proTRH 178-199 serum was described by Suzuki et al. (Suzuki et al., 2001). Briefly, the antiserum was characterized by radioimmunoassay using [^{125}I]Tyr^{178} proTRH 178-199 as a tracer. The working antiserum dilution is 1:4000, and the final dilution is 1:12000; ED50 is 181 pg/tube, using approximately 8000 cpm [^{125}I]Tyr^{178} proTRH 178-199 in this double antibody assay with a sensitivity of 19 pg/tube. The antiserum binds Tyr^{178} proTRH 178-199, unlabelled proTRH 178-199, as well as larger processing peptides including proTRH 160-255 and proTRH 160-199. Furthermore, electrophoretic separation of radiolabeled peptides from cultured cells or cold peptides extracted from rat PVN revealed that this antiserum recognizes four moieties of about 10, 5.6, 2.6, and 1.7 kDa, corresponding to proTRH 160-255, proTRH 160-199, proTRH 178-199 and proTRH 186-199, respectively (Nillni et al., 2001). Specificity for immunohistochemistry was assessed by preadsorbing the antiserum with the synthetic proTRH 178-199 peptide at the molar ratio of 1:1, 1:10, and 1:100 (immunoglobulin: proTRH 178-199 peptide). No positive immunostaining was observed in any of the preadsorption controls (Suzuki et al., 2001).

Antiserum to TRH was characterized by Lechan and Jackson (Lechan and Jackson, 1982), showing that by radioimmunoassay it can be used at a titer of 1:4800 and gives a sensitivity of 4pg/tube. The specificity of the immunohistochemical staining was assessed by saturating the TRH antiserum with 10^{-5}M synthetic TRH that resulted in the complete loss of immunostaining (Lechan and Jackson, 1982). Preincubation with a fragment of TRH (DKP), which shares two amino acids with TRH, had no effect on TRH immunostaining. In addition, the specificities of proTRH178-199 and TRH antisera are also confirmed by the fact that the two different antiserum labeled identical patterns of fibers in normal animals, and fibers as well as perikarya in colchicine-treated brains.

Results

PHAL injection sites

To map the projection fields of aPVN TRH neurons, PHAL was injected into the aPVN. In four animals, the core of the injection site covered the aPVN. In two of the four brains, cases 116 and 117, the PHAL injection site was centered halfway between the fornix and the third ventricle, corresponding to the lateral border of the aPVN (Fig. 2 A, B). In these cases, the large cores of PHAL injections substantially overlapped with the location of TRH neurons in both the aPVN and perifornical area. In case 124, PHAL was injected adjacent to the third ventricle, resulting in an injection site almost entirely confined to the aPVN and the anterior part of the periventricular parvocellular subdivision of the PVN (pPVN) (Fig. 2 C). In case 125, the PHAL injection site covered the ventral part of the aPVN and the adjacent area (Fig. 2 D).

Distribution of double-labeled PHAL/proTRH-IR fibers projecting from the aPVN/ perifornical area (cases 116 and 117)

The distribution of PHAL/proTRH fibers was very similar in both cases. PHAL/proTRH fibers were found primarily on the ipsilateral side, but some scattered double-labeled fibers were also observed on the contra-lateral side in every major projection area. The contra-lateral projection was most profound in the lateral septal nucleus. The distribution pattern of PHAL/proTRH axons in case 117 is illustrated in Fig. 3, while the relative density of double-labeled fibers in brain areas is summarized in Table 2.

Hypothalamus and preoptic region—The density of PHAL/proTRH-IR fibers was moderate in the preoptic region and anterior hypothalamus (Fig. 3 E-G). Double-labeled fibers were distributed broadly in these areas, extending to the medial preoptic nucleus (Fig. 4 C), antero-dorsal preoptic nucleus, the strial part of the preoptic area, periventricular nucleus, antero-ventral periventricular nucleus, the posterior part of the medial preoptic area, and to the most anterior portions of the anterior hypothalamic area. Laterally, the dorsal part of the lateral hypothalamic area also contained PHAL/proTRH fibers.

More caudally in the hypothalamus, a high density of double-labeled axons was found throughout the the retrochiasmatic area and the rostro-caudal extent of the arcuate nucleus (Fig. 3 H-K). The majority of double-labeled fibers were distributed in the dorsomedial part of the arcuate nucleus, whereas a moderate density of fibers was observed in the lateral part of the nucleus, with only scattered fibers in its ventromedial part. In the dorsomedial part, the double-labeled fibers were oriented mainly rostro-caudally and frequently established large varicosities (Fig. 4 A).

A large number of PHAL/proTRH-IR axons were found in the ventromedial nucleus (Fig. 3 H, I). The double-labeled fibers distributed primarily in the dorsomedial and medial parts of the nucleus. Several fibers ran parallel to the coronal plane and established several varicosities (Fig. 4 E). Many double-labeled axons were also seen immediately rostral to the ventromedial nucleus, in the medial part of the subparaventricular zone. Several varicose PHAL/proTRH-IR axons were present between the arcuate and ventromedial nuclei, and between the borders of the ventromedial and dorsomedial nuclei. Double-labeled fibers were also observed in the ventromedial part of the dorsomedial nucleus (Figs. 3 I and 4 B), rostral to the level of the compact part. More caudally, some double-labeled fibers were present in the compact part and in the ventral part of the dorsomedial nucleus.

Several PHAL/proTRH-IR fibers were distributed in a broad region ventral to the fornix (Fig. 3 H-J). This region included the tuber cinereum area, the medial tuberal nucleus (Fig. 4

F) and the ventral premammillary nucleus. PHAL/proTRH-IR fibers were also found close to the ventral surface of the hypothalamus.

Besides these major hypothalamic areas, scattered PHAL/proTRH fibers were seen in several other hypothalamic nuclei, namely the latero-anterior hypothalamic nucleus, suprachiasmatic nucleus, supraoptic nucleus, paraventricular nucleus, posterior part of the lateral hypothalamic area, posterior hypothalamic area, ventral tuberomammillary nucleus and supramammilary nucleus.

Thalamus and epithalamus—A moderate density of PHAL/proTRH-IR fibers was found in the paraventricular nucleus of the thalamus, throughout its rostro-caudal extent (Figs. 3 H, I and 4 D). These fibers mainly ran parallel to the coronal plane. Scattered PHAL/proTRH-IR axons were present in the nucleus reuniens, mediodorsal nucleus, and lateral habenular nucleus.

Substantia innominata, amygdala and hippocampus—Some varicose double-labeled fibers and medio-laterally running thin PHAL/proTRH axons that established a few boutons were observed in the substantia innominata (Figs. 3 G and 4 M). Varicose PHAL/proTRH-IR fibers were present in the medial and capsular part of the central amygdaloid nucleus (Figs. 3 L and 4 L), especially between antero-posterior levels 1.7 and 2.2 mm caudal to the Bregma. A high density of varicose PHAL/proTRH-IR axons was found in the medial amygdaloid nucleus, primarily in the posterodorsal and posteroventral subnuclei (Fig. 3 M, N). These fibers were highly varicose and many long fibers could be seen running parallel to the coronal plane (Fig. 4 J). A moderate density of double-labeled fibers was also present in the intraamygdaloid division of the bed nucleus of the stria terminalis (Fig. 3 M). More caudally several PHAL/proTRH-IR axons were observed in a dense network of proTRH-IR fibers located in the amygdalohippocampal transition area (Fig. 3 P). These PHAL/proTRH axons ran parallel to the coronal plane and established several medium to large varicosities (Fig. 4 G). Several double-labeled axons were found in a discrete group of varicose proTRH-IR fibers medial to the amygdalohippocampal transition area near the dentate gyrus (Fig. 3 O). PHAL/proTRH fibers were also present diffusely in the ventral hippocampus. Scattered PHAL/proTRH fibers were present in several areas, including the anterior cortical amydaloid nucleus, posteromedial and posterolateral cortical amygdaloid nuclei, basomedial amygdaloid nucleus, piriform cortex, ventromedial part of the lateral amygdaloid nucleus and in the fimbria of the hippocampus.

Bed nucleus of the stria terminalis and septum—PHAL/proTRH fibers were found in several divisions of the bed nucleus of the stria terminalis. Many of these fibers could be followed for a long distance indicating the coronal orientation of the fibers. High density of double-labeled fibers was present throughout the medial division (Figs. 3 C-F and 4 K). Among the nuclei of the lateral division, only the ventral and the posterior part contained significant number of double-labeled fibers (Fig. 3 E, F). In the stria terminalis, passing PHAL/proTRH fibers establishing some boutons were observed. In the lateral septal nucleus, proTRH-IR fibers established an extremely dense fiber network, frequently forming basket-like structures around the surface of perikarya and completely insheathed dendrites. Varicose PHAL/proTRH-IR axons were densely distributed in the ventral part of the lateral septal nucleus, some of them forming basket-like shapes (Figs. 3 A-E and 4 H, I). The intermediate part of the lateral septal nucleus contained a moderate number of double-labeled fibers (Fig. 3 B-D); in its medial part double-labeled axons frequently ran dorsally establishing a few en-passant boutons. The dorsal part of the lateral septal nucleus contained only scattered double-labeled fibers in its most anterior portions.

Other forebrain regions—Scattered double-labeled fibers were found in the ventral pallidum, medial septal nucleus, nucleus of the horizontal limb of the diagonal band, nucleus of the vertical limb of the diagonal band, major island of Calleja, posterior part of the anterior olfactory nucleus, and in the area adjacent dorsomedially to the dorsal endopiriform nucleus.

Midbrain and hindbrain—Some scattered PHAL/proTRH-IR fibers could be observed in the periaqueductal gray, lateral and ventrolateral periaqueductal gray, ventral tegmental area and the central part of the lateral parabrachial nucleus.

Cases 124 and 125

Despite the apparently limited spread of the tracer outside the aPVN, the distribution pattern of PHAL/proTRH axons in case 124 was very similar to cases 116 and 117, with only slight differences in the density of double-labeled fibers in some regions. In case 125, the general distribution of double-labeled axons showed similarities with the pattern seen in the brains described above. However, generally fewer PHAL/proTRH axons were observed in all regions, and only sparse double-labeled axons were present in the medial amygdaloid nucleus, dorsomedial nucleus and substantia innominata. No PHAL/proTRH fibers were observed near the dentate gyrus and in the ventral hippocampus.

Distribution of retrogradely-labeled TRH-IR cell bodies in the aPVN and perifornical area—To differentiate between the projection sites of TRH neurons residing in the aPVN and perifornical area, the retrograde tracer, CTB, was injected into brain regions where high or moderate density of the PHAL/proTRH-IR fibers were observed in the anterograde tracing experiment. Representative CTB injection sites are shown in Fig. 5. CTB/TRH-IR neurons in the aPVN and perifornical area were found primarily ipsilateral to the injection sites, with fewer double-labeled neurons on the contralateral side. The retrogradely-labeled TRH neurons in the aPVN and perifornical region were counted in each brain with a successful CTB injection. The data are summarized in Table 3.

A moderate to high number of CTB-containing TRH neurons in the aPVN were found after CTB injections into the arcuate nucleus (Figs. 6 A and 8 A), dorsomedial nucleus (Figs. 6 C and 8 B), medial preoptic area (Figs. 6 D and 8 E), caudal tuber cinereum area (Figs. 7 D and 8 D), ventral premammillary nucleus, anterior and posterior part of the medial division of the BNST (Figs. 7 A, B and 8 J), paraventricular nucleus of the thalamus (7 E and 8 G), central amygdaloid nucleus (Figs. 7 F and 8 K) and the ventral part of the lateral septal nucleus (Fig. 8 H). Only few CTB/TRH-IR neurons, less than 10/animal, were found in the aPVN after CTB injections into the ventromedial nucleus, medial amygdaloid nucleus and the amygdalohippocampal area.

A moderate to high number of CTB-containing TRH neurons were present in the perifornical area after CTB injections into the ventral part of the lateral septal nucleus (Figs. 7 G and 8 H), ventromedial nucleus (Figs. 6 B and 8 C), dorsomedial nucleus (Figs. 6 C and 8 B), medial preoptic region (Figs. 6 D and 8 E), medial amygdaloid nucleus (Fig. 8 F), amygdalohippocampal area (Figs. 6 E and 8 I), ventral premammillary nucleus and the posterior part of the medial division of the BNST (Figs. 7 A, C and 8 J). The greatest number of retrogradely labeled TRH neurons were present in the perifornical area after CTB injection into the ventral part of the lateral septal nucleus. Only rare (less than 10/animal) perifornical TRH neurons contained CTB when injections were made into the arcuate nucleus, paraventricular nucleus of the thalamus, central amygdaloid nucleus, caudal part of the tuber cinereum area and anterior part of the medial division of the BNST.

In all of the CTB-injected brains, very few TRH neurons in hypophysiotropic parts of the PVN contained CTB. In the medial and periventricular parvocellular subdivisions, 10 or more CTB-IR TRH neurons/animal were found in only two cases: after CTB injection into the medial preoptic region (10 neurons) and the dorsomedial nucleus (12 neurons).

Discussion

In the present study we identified major efferent projection sites of the non-hypophysiotropic population of TRH neurons located in the aPVN by using combined anterograde and retrograde tract-tracing methods. Additionally, we identified the main projection fields of an adjacent population of TRH neurons located in the perifornical area. Although the two TRH neuronal populations partially overlap, their projection fields substantially differ, suggesting different physiological roles for these two cell populations. As a common trait, both cell groups innervate hypothalamic and extrahypothalamic forebrain nuclei and do not send a substantial projection to the hindbrain, suggesting that they regulate homeostatic and behavioral functions rather at the level of the hypothalamus and the limbic forebrain. Table 4 summarizes the identified projection fields of aPVN and perifornical TRH neurons.

Technical considerations

Mapping the projection sites of aPVN TRH neurons by anterograde tract-tracing was complicated by the small volume of the aPVN and the close proximity of perifornical TRH neurons, and made difficult the selective targeting of TRH neurons residing in the aPVN TRH neurons. Indeed, even PHAL injections that appeared confined mostly to the aPVN resulted in a qualitatively similar topography of PHAL/proTRH fibers when compared to those cases in which PHAL cores overlapped both the aPVN and the medial part of the perifornical area, raising the possibility that perifornical TRH neurons may take up PHAL from the aPVN through dendrites that may penetrate the aPVN. Therefore, it was necessary to conduct retrograde tracing experiments in order to distinguish between the genuine projection sites of TRH neurons residing in the aPVN and perifornical area.

CTB injections into several regions where a relative abundance of PHAL/proTRH axons were found revealed distinct projection sites of aPVN and perifornical TRH neurons, albeit common projection fields were also found. Although the extent of the projections from the aPVN and perifornical group to each specific area cannot be quantitatively compared, the arcuate nucleus would appear to be the primary target of the aPVN, whereas the lateral septal nucleus appears to the be primary target of perifornical TRH neurons. In the anterograde tracing experiment, a high density of PHAL/proTRH fibers was observed in the arcuate nucleus, and a large number of TRH neurons in the aPVN but not the perifornical area were labeled retrogradely from the arcuate nucleus. In contrast, the ventral part of the lateral septal nucleus contained a high density of PHAL/proTRH fibers, and after CTB injection, a large number of TRH neurons in the perifornical area but not the aPVN were retrogradely labeled. Projections of perifornical TRH neurons to the lateral septal area were also reported in earlier studies by Ishikawa et al. and Merchenthaler (Ishikawa et al., 1986; Merchenthaler, 1991).

It should be noted that CTB was injected into most of the regions where high to moderate density of anterogradely labeled proTRH-containing fibers were observed, but it was beyond the scope of this study to inject CTB into regions where only a low density of PHAL/TRH fibers were observed. Thus, it is conceivable that there might be additional brain areas that receive functionally significant, but less dense innervation of TRH-containing axons originating from the aPVN and/or perifornical areas. Furthermore, PHAL injections covered

only the medial part of the perifornical TRH cell group. Thus, there may be additional projection sites of this cell group that were not observed in our study.

Functional implications

There is essentially nothing known about the biological significance of TRH neurons located in the aPVN. Nevertheless, the robust innervation of these cells by AGRP/NPY and α-MSH/CART neurons of the arcuate nucleus (Fekete et al., 2000a; Legradi and Lechan, 1999) is indicative of the possibility that aPVN TRH neurons may be tightly regulated by feeding-related neuronal afferents and integrated into the energy control system. Indeed, TRH is well known to regulate appetite and when injected into the brain it consistently reduces food intake and the time spent interacting with food in all animals species studied (Horita, 1998; Morley, 1980; Steward et al., 2003; Suzuki et al., 1982; Vijayan and McCann, 1977; Vogel et al., 1979). This includes a reduction in food intake in *ad lib* feeding animals, animals that have been subjected to a fast and reintroduced to food, and models of stress-induced eating. Given that the major projection fields of aPVN TRH neurons include the arcuate and dorsomedial nuclei, two critical integrating centers in the brain involved in the regulation of food intake (Morton et al., 2006), it is conceivable that the anorectic actions of TRH could be mediated through one or both of these areas. In addition, the presence of projection fields of aPVN TRH neurons to extrahypothalamic areas such as the paraventricular thalamic nucleus, central amygdaloid nucleus, bed nucleus of the stria terminalis and ventral part of the lateral septal nucleus, may integrate the regulation of appetite and satiety with other components of the energy regulatory system. For example, projections to the paraventricular thalamic nucleus may induce arousal (Van der Werf et al., 2002), and hence, increase locomotor activity, now considered an important component of energy homeostasis (Castaneda et al., 2005). Projections to the bed nucleus of the stria terminalis and central amygdaloid nucleus may contribute to feeding behavior (Dong et al., 2001; Ju and Swanson, 1989; Kelley, 2004) and/or induce gastric contractility (Morrow et al., 1996).

Nevertheless, the major projection field of aPVN TRH neurons in the arcuate nucleus is primarily the dorsomedial part of the nucleus, a region not generally associated with the regulation of food-related signals, but rather with the regulation of prolactin secretion via dopamine-producing neurons of the tuberoinfundibular system (Freeman et al., 2000). TRH has a well known effect on prolactin secretion, potently releasing prolactin from anterior pituitary lactotrophs (Dannies and Tashjian, 1974). However, proTRH178-199, a non-TRH peptide derived from the post-translational processing of the TRH prohormone (Nillni and Sevarino, 1999), also has a potent effect on prolactin secretion by decreasing the expression of the dopamine-synthesizing enzyme, tyrosine-hydroxylase when injected to the arcuate nucleus (Goldstein et al., 2007). Thus, TRH neurons may have a dual action on prolactin secretion, both through direct effects on lactrotrophs and indirect effects by inhibiting the tuberoinfundibular dopaminergic system.

By projecting to the preoptic area, aPVN TRH neurons may also be involved in the regulation of thermogenesis. Injection of TRH into the preoptic area inhibits heat-sensitive neurons and activates cold-sensitive neurons (Hori et al., 1988). This action results in increased body temperature through peripheral vasoconstriction, increased metabolic heat production and shivering (Chi and Lin, 1983). Thus, it is intriguing to consider the possibility that activation of aPVN TRH neurons following a meal may contribute to the generation of diet-induced thermogenesis in coordination with other TRH-mediated responses associated with meal termination. Alternatively, this projection pathway may be involved in the adaptation response to cold stress, given that animals exposed to a cold environment increase TRH gene expression in all PVN regions including the aPVN (Sanchez et al., 2001). Thus, it is possible that cold-sensitive TRH neurons in the PVN not only increase heat production by increasing peripheral thyroid hormone levels (Bianco et al.,

2002; Zoeller et al., 1990), but also by regulating preoptic neurons that increase heat production via the activation of the sympathetic nervous system (Morrison et al., 2008).

Projections of aPVN TRH neurons to the dorsomedial nucleus could also contribute to some of the well-recognized autonomic effects of centrally administered TRH (Nillni and Sevarino, 1999), particularly those involved in the regulation of the cardiovascular and respiratory systems. Activation of the DMN increases heart rate, and vasomotor activity and induces hyperventilation (Horiuchi et al., 2006; McDowall et al., 2007), responses that are highly reminiscent of the central actions of TRH (Nillni and Sevarino, 1999). Many of the central effects of TRH on the autonomic system, however, are thought to be exerted directly on the brainstem (Nillni and Sevarino, 1999), and/or through projections of TRH-producing neurons in the medullary raphe to preganglionic sympathetic neurons in the spinal cord (Nillni and Sevarino, 1999). Studies involving focal, intranuclear injections of TRH into the DMN will be required to determine whether this region also contributes to the actions of TRH on autonomic function.

Although effects of TRH or proTRH-derived peptides on sexual behavior has not been described, projections to the medial preoptic area/medial preoptic nucleus and to the ventral premammillary nucleus raise the possibility that aPVN TRH neurons could be involved in the regulation of reproductive functions. The medial preoptic area has a critical role in sexual behaviour (Balthazart and Ball, 2007), whereas the ventral premammillary nucleus has been shown to be activated by pheromonal stimuli (Cavalcante et al., 2006; Yokosuka et al., 1999) and it possesses bidirectional connections with several nuclei related to reproductive control (Canteras et al., 1992). Innervation of these nuclei by TRH neurons in the aPVN may serve to coordinate sexual behavior with the nutritional status of the animal.

While not a primary objective of this study, the major projection sites of the TRH neurons residing in the rostral part of the perifornical area were also identified. Contrary to aPVN TRH neurons, perifornical TRH neurons were found to densely innervate the ventromedial nucleus, especially its dorsomedial part. This region of the ventromedial nucleus was shown by Elmquist et al. (Elmquist et al., 1998) to express leptin receptors and to be activated by circulating leptin (Elias et al., 2000; Elmquist et al., 1997). As selective removal of leptin receptors from these neurons results in increased fat mass and body weight (Dhillon et al., 2006), it is possible that perifornical TRH neurons also have important regulatory effects on energy homeostasis.

A major difference between the projections of aPVN and perifornical TRH neurons, however, is that perifornical TRH neurons project more extensively to extrahypothalamic limbic areas. Retrograde labeling from the ventral lateral septum suggests that almost an order of magnitude more TRH neurons project to the lateral septum from the perifornical area than from the aPVN. In addition, perifornical TRH neurons densely innervate the medial amygdaloid nucleus and amygdalohippocampal area. These regions are involved in the regulation of a variety of behaviors including sexual behavior, feeding behavior, aggression, coping with stressful situations, and in emotional responses (Bakshi et al., 2007; Ciccocioppo et al., 2003; Fujisaki et al., 2004; Hahn and Coen, 2006; Heeb and Yahr, 1996; Herman et al., 2005; King, 2006; Kollack-Walker et al., 1997; Koolhaas et al., 1998; Simerly et al., 1990). Given that the endogenous TRH system plays key role in regulating anxiety and depression in rodents (Zeng et al., 2007) and that TRH also has anti-depressant effects in humans (Callahan et al., 1997; Kastin et al., 1972; Prange et al., 1972), perifornical TRH neurons may be involved in mood regulation. A role of perifornical TRH neurons in sexual behavior and the hypothalamic-pituitary-gonadal axis is also suggested by their projections to the medial preoptic region, ventral premammillary nucleus and a narrow zone between the dorsomedial and ventromedial nuclei. The latter region has been

implicated in regulation of the hypothalamic-pituitary-gonadal axis *via* RF-amide-related peptide expressing neurons in this region (Hinuma et al., 2000; Liu et al., 2001) that inhibit gonadotropin release (Kriegsfeld et al., 2006).

In summary, projection fields of aPVN TRH neurons raise the possibility that this non-hypophysiotropic TRH cell population may influence energy homeostasis, thermoregulation, prolactin synthesis and possibly sexual function. In contrast, perifornical TRH neurons may primarily be involved in regulation of limbic functions and therefore, functionally different than aPVN TRH neurons. Partially overlapping projections of the TRH neurons from both regions, and in particular, the heavy innervation to the ventromedial nucleus, potentially implicates at least a subpopulation of perifornical TRH neurons in the control of food intake. These studies provide important initial data from which physiological studies can be designed to further understand the potential role of these cell groups in the regulation of neuroendocrine function.

Acknowledgments

The authors are grateful to Drs. Éva Rédei and Ivor M. Jackson for the generous gift of primary antisera. The expert technical assistance of Éva Laki, Andrea Kádár and Ágnes Simon is greatly appreciated.

This work was supported by grants from the Sixth EU Research Framework Programme (contract LSHM-CT-2003-503041) and NIH (DK37021, RDK070600 and TW007834).

Abbreviations

ac	Anterior comissure
aca	Anterior comissure, anterior part
Acb	Accumbens nucleus
AHi	amygdalohippocampal area
aPVN	Paraventricular hypothalamic nucleus, anterior parvocellular subdivision
Arc	Arcuate nucleus
ArcL	Arcuate nucleus, lateral part
ArcM	Arcuate nucleus, medial part
AVPe	Anteroventral periventricular nucleus
BSTIA	Bed nucleus of the stria terminalis, intraamygdaloid division
BSTL	Bed nucleus of the stria terminalis, lateral division
BSTLV	Bed nucleus of the stria terminalis, lateral division, ventral part
BSTM	Bed nucleus of the stria terminalis, medial division
BSTMA	Bed nucleus of the stria terminalis, medial division, anterior part
cc	Corpus callosum
CeA	Central amygdaloid nucleus
cst	Commissural stria terminalis
DG	dentate gyrus
DMN	Dorsomedial hypothalamic nucleus
f	Fornix

fi	fimbria of the hippocampus
fr	Fasciculus retroflexus
HDB	Nucleus of the horizontal limb of the diagonal band
I	Intercalated nuclei of the amygdala
ic	Internal capsule
ICjM	Islands of Calleja, major island
LH	Lateral hypothalamic area
LPO	Lateral preoptic area
LSD	Lateral septal nucleus, dorsal part
LSI	Lateral septal nucleus, intermediate part
LSV	Lateral septal nucleus, ventral part
MeAD	Medial amygdaloid nucleus, anterodorsal part
MePD	Medial amygdaloid nucleus, posterodorsal part
MePV	Medial amygdaloid nucleus, posteroventral part
MPA	Medial preoptic area
MPO	Medial preoptic nucleus
mPVN	Paraventricular hypothalamic nucleus, medial parvocellular subdivision
MS	Medial septal nucleus
mt	Mammillothalamic tract
MTu	Medial tuberal nucleus
opt	Optic tract
ox	Optic chiasm
Pe	Periventricular hypothalamic nucleus
Pf	Perifornical area
pm	Principal mammillary tract
PMV	Ventral premammillary nucleus
pPVN	Paraventricular hypothalamic nucleus, periventricular parvocellular subdivision
PV	Paraventricular thalamic nucleus
PVA	Paraventricular thalamic nucleus, anterior part
RCh	Retrochiasmatic area
SCh	Suprachiasmatic nucleus
SI	Substantia innominata
sm	Stria medullaris of the thalamus
sox	Supraoptic decussation
st	Stria terminalis

TC	Tuber cinereum area
VDB	Nucleus of the vertical limb of the diagonal band
VMN	Ventromedial hypothalamic nucleus

References

Bakshi VP, Newman SM, Smith-Roe S, Jochman KA, Kalin NH. Stimulation of lateral septum CRF2 receptors promotes anorexia and stress-like behaviors: functional homology to CRF1 receptors in basolateral amygdala. J Neurosci. 2007; 27(39):10568–10577. [PubMed: 17898228]

Balthazart J, Ball GF. Topography in the preoptic region: differential regulation of appetitive and consummatory male sexual behaviors. Front Neuroendocrinol. 2007; 28(4):161–178. [PubMed: 17624413]

Bianco AC, Salvatore D, Gereben B, Berry MJ, Larsen PR. Biochemistry, cellular and molecular biology, and physiological roles of the iodothyronine selenodeiodinases. Endocr Rev. 2002; 23(1): 38–89. [PubMed: 11844744]

Callahan AM, Frye MA, Marangell LB, George MS, Ketter TA, L'Herrou T, Post RM. Comparative antidepressant effects of intravenous and intrathecal thyrotropin-releasing hormone: confounding effects of tolerance and implications for therapeutics. Biol Psychiatry. 1997; 41(3):264–272. [PubMed: 9024949]

Canteras NS, Simerly RB, Swanson LW. Projections of the ventral premammillary nucleus. J Comp Neurol. 1992; 324(2):195–212. [PubMed: 1430329]

Castaneda TR, Jurgens H, Wiedmer P, Pfluger P, Diano S, Horvath TL, Tang-Christensen M, Tschop MH. Obesity and the neuroendocrine control of energy homeostasis: the role of spontaneous locomotor activity. J Nutr. 2005; 135(5):1314–1319. [PubMed: 15867332]

Cavalcante JC, Bittencourt JC, Elias CF. Female odors stimulate CART neurons in the ventral premammillary nucleus of male rats. Physiol Behav. 2006; 88(1-2):160–166. [PubMed: 16687159]

Chi ML, Lin MT. Involvement of adrenergic receptor mechanisms within hypothalamus in the fever induced by amphetamine and thyrotropin-releasing hormone in the rat. J Neural Transm. 1983; 58(3-4):213–222. [PubMed: 6420515]

Ciccocioppo R, Fedeli A, Economidou D, Policani F, Weiss F, Massi M. The bed nucleus is a neuroanatomical substrate for the anorectic effect of corticotropin-releasing factor and for its reversal by nociceptin/orphanin FQ. J Neurosci. 2003; 23(28):9445–9451. [PubMed: 14561874]

Dannies PS, Tashjian AH Jr. Pyroglutamyl-histidyl-prolineamide (TRH). A neurohormone which affects the release and synthesis of prolactin and thyrotropin. Isr J Med Sci. 1974; 10(10):1294–1304. [PubMed: 4215776]

Dhillon H, Zigman JM, Ye C, Lee CE, McGovern RA, Tang V, Kenny CD, Christiansen LM, White RD, Edelstein EA, Coppari R, Balthasar N, Cowley MA, Chua S Jr. Elmquist JK, Lowell BB. Leptin directly activates SF1 neurons in the VMH, and this action by leptin is required for normal body-weight homeostasis. Neuron. 2006; 49(2):191–203. [PubMed: 16423694]

Dong HW, Petrovich GD, Swanson LW. Topography of projections from amygdala to bed nuclei of the stria terminalis. Brain Res Brain Res Rev. 2001; 38(1-2):192–246. [PubMed: 11750933]

Elias CF, Kelly JF, Lee CE, Ahima RS, Drucker DJ, Saper CB, Elmquist JK. Chemical characterization of leptin-activated neurons in the rat brain. J Comp Neurol. 2000; 423(2):261–281. [PubMed: 10867658]

Elmquist JK, Ahima RS, Maratos-Flier E, Flier JS, Saper CB. Leptin activates neurons in ventrobasal hypothalamus and brainstem. Endocrinology. 1997; 138(2):839–842. [PubMed: 9003024]

Elmquist JK, Bjorbaek C, Ahima RS, Flier JS, Saper CB. Distributions of leptin receptor mRNA isoforms in the rat brain. J Comp Neurol. 1998; 395(4):535–547. [PubMed: 9619505]

Fekete C, Legradi G, Mihaly E, Huang QH, Tatro JB, Rand WM, Emerson CH, Lechan RM. alpha-Melanocyte-stimulating hormone is contained in nerve terminals innervating thyrotropin-releasing hormone-synthesizing neurons in the hypothalamic paraventricular nucleus and prevents fasting-

induced suppression of prothyrotropin-releasing hormone gene expression. J Neurosci. 2000a; 20(4):1550–1558. [PubMed: 10662844]

Fekete C, Mihály M, Luo LG, Kelly J, Clausen JT, Q. M, Rand WM, Moss LG, Kuhar M, Emerson CH, Jackson IMD, Lechan RM. Association of CART-immunoreactive elements with thyrotropin-releasing hormone-synthesizing neurons in the hypothalamic paraventricular nucleus and its role in the regulation of the hypothalamic-pituitary-thyroid axis during fasting. J Neurosci. 2000b; 20:9224–9234. [PubMed: 11125000]

Freeman ME, Kanyicska B, Lerant A, Nagy G. Prolactin: structure, function, and regulation of secretion. Physiol Rev. 2000; 80(4):1523–1631. [PubMed: 11015620]

Fujisaki M, Hashimoto K, Iyo M, Chiba T. Role of the amygdalo-hippocampal transition area in the fear expression: evaluation by behavior and immediate early gene expression. Neuroscience. 2004; 124(1):247–260. [PubMed: 14960356]

Goldstein J, Perello M, Nillni EA. PreproThyrotropin-releasing hormone 178-199 affects tyrosine hydroxylase biosynthesis in hypothalamic neurons: a possible role for pituitary prolactin regulation. J Mol Neurosci. 2007; 31(1):69–82. [PubMed: 17416971]

Hahn JD, Coen CW. Comparative study of the sources of neuronal projections to the site of gonadotrophin-releasing hormone perikarya and to the anteroventral periventricular nucleus in female rats. J Comp Neurol. 2006; 494(1):190–214. [PubMed: 16304687]

Heeb MM, Yahr P. c-Fos immunoreactivity in the sexually dimorphic area of the hypothalamus and related brain regions of male gerbils after exposure to sex-related stimuli or performance of specific sexual behaviors. Neuroscience. 1996; 72(4):1049–1071. [PubMed: 8735229]

Herman JP, Ostrander MM, Mueller NK, Figueiredo H. Limbic system mechanisms of stress regulation: hypothalamo-pituitary-adrenocortical axis. Prog Neuropsychopharmacol Biol Psychiatry. 2005; 29(8):1201–1213. [PubMed: 16271821]

Hinuma S, Shintani Y, Fukusumi S, Iijima N, Matsumoto Y, Hosoya M, Fujii R, Watanabe T, Kikuchi K, Terao Y, Yano T, Yamamoto T, Kawamata Y, Habata Y, Asada M, Kitada C, Kurokawa T, Onda H, Nishimura O, Tanaka M, Ibata Y, Fujino M. New neuropeptides containing carboxy-terminal RFamide and their receptor in mammals. Nat Cell Biol. 2000; 2(10):703–708. [PubMed: 11025660]

Hori T, Yamasaki M, Asami T, Koga H, Kiyohara T. Responses of anterior hypothalamic-preoptic thermosensitive neurons to thyrotropin releasing hormone and cyclo(His-Pro). Neuropharmacology. 1988; 27(9):895–901. [PubMed: 3141827]

Horita A. An update on the CNS actions of TRH and its analogs. Life Sci. 1998; 62(17-18):1443–1448. [PubMed: 9585116]

Horiuchi J, McDowall LM, Dampney RA. Differential control of cardiac and sympathetic vasomotor activity from the dorsomedial hypothalamus. Clin Exp Pharmacol Physiol. 2006; 33(12):1265–1268. [PubMed: 17184513]

Ishikawa K, Taniguchi Y, Inoue K, Kurosumi K, Suzuki M. Immunocytochemical delineation of thyrotrophic area: origin of thyrotropin-releasing hormone in the median eminence. Neuroendocrinology. 1988; 47(5):384–388. [PubMed: 3135505]

Ishikawa K, Taniguchi Y, Kurosumi K, Suzuki M. Origin of septal thyrotropin-releasing hormone in the rat. Neuroendocrinology. 1986; 44(1):54–58. [PubMed: 3097562]

Ju G, Swanson LW. Studies on the cellular architecture of the bed nuclei of the stria terminalis in the rat: I. Cytoarchitecture. J Comp Neurol. 1989; 280(4):587–602. [PubMed: 2708568]

Kastin AJ, Ehrensing RH, Schalch DS, Anderson MS. Improvement in mental depression with decreased thyrotropin response after administration of thyrotropin-releasing hormone. Lancet. 1972; 2(7780):740–742. [PubMed: 4116150]

Kawano H, Tsuruo Y, Bando H, Daikoku S. Hypophysiotrophic TRH-producing neurons identified by combining immunohistochemistry for pro-TRH and retrograde tracing. J Comp Neurol. 1991; 307(4):531–538. [PubMed: 1907979]

Kelley AE. Ventral striatal control of appetitive motivation: role in ingestive behavior and reward-related learning. Neurosci Biobehav Rev. 2004; 27(8):765–776. [PubMed: 15019426]

King BM. Amygdaloid lesion-induced obesity: relation to sexual behavior, olfaction, and the ventromedial hypothalamus. Am J Physiol Regul Integr Comp Physiol. 2006; 291(5):R1201–1214. [PubMed: 16778067]

Kollack-Walker S, Watson SJ, Akil H. Social stress in hamsters: defeat activates specific neurocircuits within the brain. J Neurosci. 1997; 17(22):8842–8855. [PubMed: 9348352]

Koolhaas JM, Everts H, de Ruiter AJ, de Boer SF, Bohus B. Coping with stress in rats and mice: differential peptidergic modulation of the amygdala-lateral septum complex. Prog Brain Res. 1998; 119:437–448. [PubMed: 10074805]

Kriegsfeld LJ, Mei DF, Bentley GE, Ubuka T, Mason AO, Inoue K, Ukena K, Tsutsui K, Silver R. Identification and characterization of a gonadotropin-inhibitory system in the brains of mammals. Proc Natl Acad Sci U S A. 2006; 103(7):2410–2415. [PubMed: 16467147]

Lechan RM. Update on thyrotropin-releasing hormone. Thyroid Today. 1993; 16(1):1–12.

Lechan RM, Jackson IM. Immunohistochemical localization of thyrotropin-releasing hormone in the rat hypothalamus and pituitary. Endocrinology. 1982; 111(1):55–65. [PubMed: 6806077]

Lechan RM, Segerson TP. Pro-TRH gene expression and precursor peptides in rat brain. Observations by hybridization analysis and immunocytochemistry. Ann N Y Acad Sci. 1989; 553:29–59. [PubMed: 2497675]

Legradi G, Lechan RM. Agouti-related protein containing nerve terminals innervate thyrotropin-releasing hormone neurons in the hypothalamic paraventricular nucleus. Endocrinology. 1999; 140(8):3643–3652. [PubMed: 10433222]

Liu Q, Guan XM, Martin WJ, McDonald TP, Clements MK, Jiang Q, Zeng Z, Jacobson M, Williams DL Jr. Yu H, Bomford D, Figueroa D, Mallee J, Wang R, Evans J, Gould R, Austin CP. Identification and characterization of novel mammalian neuropeptide FF-like peptides that attenuate morphine-induced antinociception. J Biol Chem. 2001; 276(40):36961–36969. [PubMed: 11481330]

McDowall LM, Horiuchi J, Dampney RA. Effects of disinhibition of neurons in the dorsomedial hypothalamus on central respiratory drive. Am J Physiol Regul Integr Comp Physiol. 2007; 293(4):R1728–1735. [PubMed: 17715179]

Merchenthaler I. Co-localization of enkephalin and TRH in perifornical neurons of the rat hypothalamus that project to the lateral septum. Brain Res. 1991; 544(1):177–180. [PubMed: 1713116]

Merchenthaler I, Liposits Z. Mapping of thyrotropin-releasing hormone (TRH) neuronal systems of rat forebrain projecting to the median eminence and the OVLT. Immunocytochemistry combined with retrograde labeling at the light and electron microscopic levels. Acta Biol Hung. 1994; 45(2-4): 361–374. [PubMed: 7725828]

Morley JE. The neuroendocrine control of appetite: the role of the endogenous opiates, cholecystokinin, TRH, gamma-amino-butyric-acid and the diazepam receptor. Life Sci. 1980; 27(5):355–368. [PubMed: 6774182]

Morrison SF, Nakamura K, Madden CJ. Central control of thermogenesis in mammals. Exp Physiol. 2008; 93(7):773–797. [PubMed: 18469069]

Morrow NS, Hodgson DM, Garrick T. Microinjection of thyrotropin-releasing hormone analogue into the central nucleus of the amygdala stimulates gastric contractility in rats. Brain Res. 1996; 735(1): 141–148. [PubMed: 8905179]

Morton GJ, Cummings DE, Baskin DG, Barsh GS, Schwartz MW. Central nervous system control of food intake and body weight. Nature. 2006; 443(7109):289–295. [PubMed: 16988703]

Nillni EA, Aird F, Seidah NG, Todd RB, Koenig JI. PreproTRH(178-199) and two novel peptides (pFQ7 and pSE14) derived from its processing, which are produced in the paraventricular nucleus of the rat hypothalamus, are regulated during suckling. Endocrinology. 2001; 142(2):896–906. [PubMed: 11159863]

Nillni EA, Sevarino KA. The biology of pro-thyrotropin-releasing hormone-derived peptides. Endocr Rev. 1999; 20(5):599–648. [PubMed: 10529897]

Nishiyama T, Kawano H, Tsuruo Y, Maegawa M, Hisano S, Adachi T, Daikoku S, Suzuki M. Hypothalamic thyrotropin-releasing hormone (TRH)-containing neurons involved in the

hypothalamic-hypophysial-thyroid axis. Light microscopic immunohistochemistry. Brain Res. 1985; 345(2):205–218. [PubMed: 3930003]

Paxinos, G.; Watson, C. The Rat Brain in Stereotaxic Coordinates. Academic Press; San Diego, CA: 1998.

Prange AJ Jr. Lara PP, Wilson IC, Alltop LB, Breese GR. Effects of thyrotropin-releasing hormone in depression. Lancet. 1972; 2(7785):999–1002. [PubMed: 4116985]

Sanchez E, Uribe RM, Corkidi G, Zoeller RT, Cisneros M, Zacarias M, Morales-Chapa C, Charli JL, Joseph-Bravo P. Differential responses of thyrotropin-releasing hormone (TRH) neurons to cold exposure or suckling indicate functional heterogeneity of the TRH system in the paraventricular nucleus of the rat hypothalamus. Neuroendocrinology. 2001; 74(6):407–422. [PubMed: 11752897]

Schwartz MW, Woods SC, Porte D Jr. Seeley RJ, Baskin DG. Central nervous system control of food intake. Nature. 2000; 404(6778):661–671. [PubMed: 10766253]

Segerson TP, Hoefler H, Childers H, Wolfe HJ, Wu P, Jackson IM, Lechan RM. Localization of thyrotropin-releasing hormone prohormone messenger ribonucleic acid in rat brain in situ hybridization. Endocrinology. 1987a; 121(1):98–107. [PubMed: 3109882]

Segerson TP, Kauer J, Wolfe HC, Mobtaker H, Wu P, Jackson IM, Lechan RM. Thyroid hormone regulates TRH biosynthesis in the paraventricular nucleus of the rat hypothalamus. Science. 1987b; 238(4823):78–80. [PubMed: 3116669]

Simerly RB, Chang C, Muramatsu M, Swanson LW. Distribution of androgen and estrogen receptor mRNA-containing cells in the rat brain: an in situ hybridization study. J Comp Neurol. 1990; 294(1):76–95. [PubMed: 2324335]

Steward CA, Horan TL, Schuhler S, Bennett GW, Ebling FJ. Central administration of thyrotropin releasing hormone (TRH) and related peptides inhibits feeding behavior in the Siberian hamster. Neuroreport. 2003; 14(5):687–691. [PubMed: 12692464]

Suzuki S, Solberg LC, Redei EE, Handa RJ. Prepro-thyrotropin releasing hormone 178-199 immunoreactivity is altered in the hypothalamus of the Wistar-Kyoto strain of rat. Brain Res. 2001; 913(2):224–233. [PubMed: 11549391]

Suzuki T, Kohno H, Sakurada T, Tadano T, Kisara K. Intracranial injection of thyrotropin releasing hormone (TRH) suppresses starvation-induced feeding and drinking in rats. Pharmacol Biochem Behav. 1982; 17(2):249–253. [PubMed: 6813881]

Van der Werf YD, Witter MP, Groenewegen HJ. The intralaminar and midline nuclei of the thalamus. Anatomical and functional evidence for participation in processes of arousal and awareness. Brain Res Brain Res Rev. 2002; 39(2-3):107–140. [PubMed: 12423763]

Vijayan E, McCann SM. Suppression of feeding and drinking activity in rats following intraventricular injection of thyrotropin releasing hormone (TRH). Endocrinology. 1977; 100(6):1727–1730. [PubMed: 404133]

Vogel RA, Cooper BR, Barlow TS, Prange AJ Jr. Mueller RA, Breese GR. Effects of thyrotropin-releasing hormone on locomotor activity, operant performance and ingestive behavior. J Pharmacol Exp Ther. 1979; 208(2):161–168. [PubMed: 105126]

Yokosuka M, Matsuoka M, Ohtani-Kaneko R, Iigo M, Hara M, Hirata K, Ichikawa M. Female-soiled bedding induced fos immunoreactivity in the ventral part of the premammillary nucleus (PMv) of the male mouse. Physiol Behav. 1999; 68(1-2):257–261. [PubMed: 10627089]

Zeng H, Schimpf BA, Rohde AD, Pavlova MN, Gragerov A, Bergmann JE. Thyrotropin-releasing hormone receptor 1-deficient mice display increased depression and anxiety-like behavior. Mol Endocrinol. 2007; 21(11):2795–2804. [PubMed: 17666589]

Zoeller RT, Kabeer N, Albers HE. Cold exposure elevates cellular levels of messenger ribonucleic acid encoding thyrotropin-releasing hormone in paraventricular nucleus despite elevated levels of thyroid hormones. Endocrinology. 1990; 127(6):2955–2962. [PubMed: 2123445]

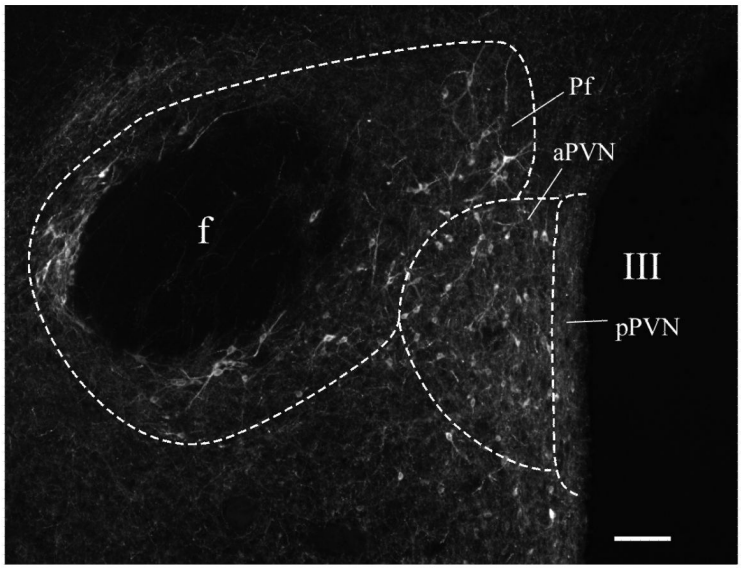

Fig. 1.
Photomicrograph of the rostral-mid level of the aPVN, where perifornical TRH neurons are in close proximity to the border of the aPVN. Scale bar 100 μm.

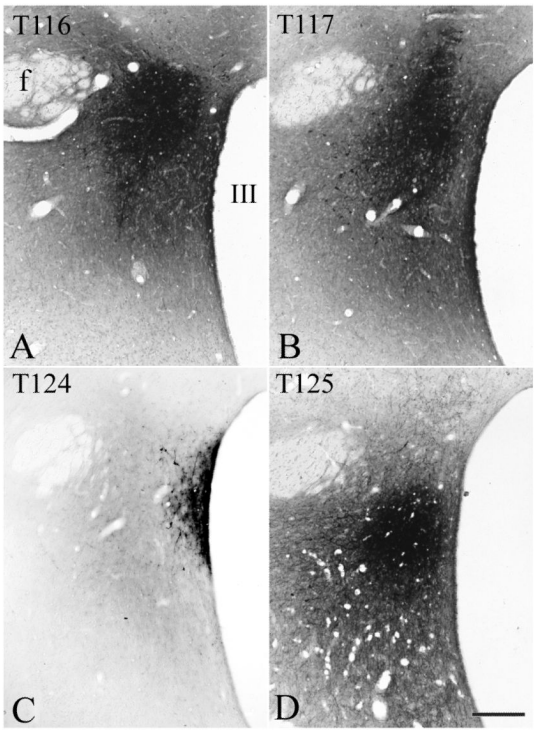

Fig. 2.
Localization of PHAL injection sites in four brains used in the anterograde tracing experiment. Scale bar shown in D corresponds to 250 μm and refers to all micrographs.

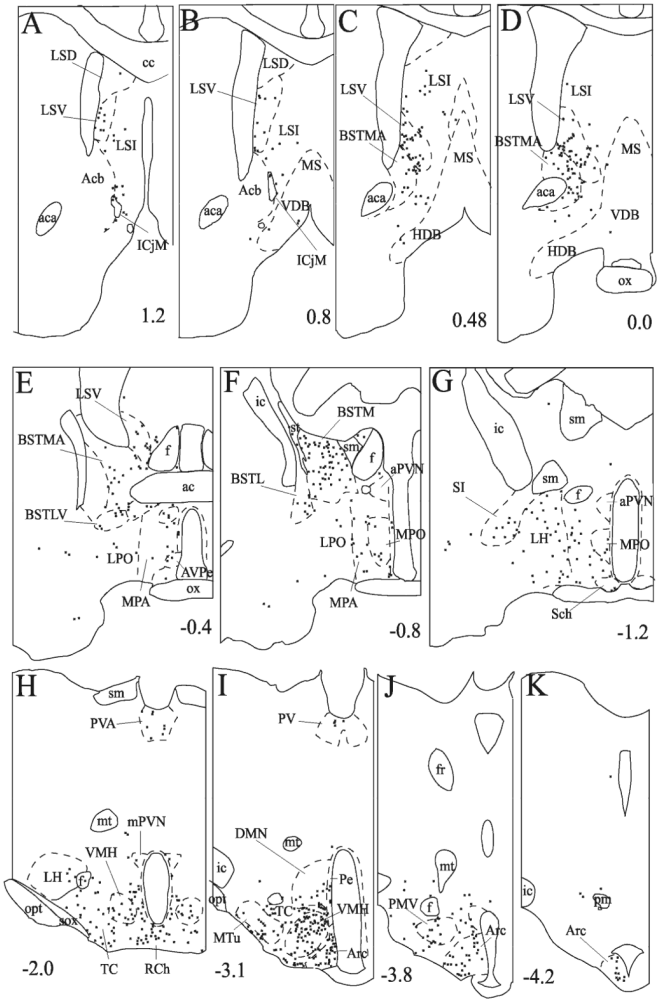

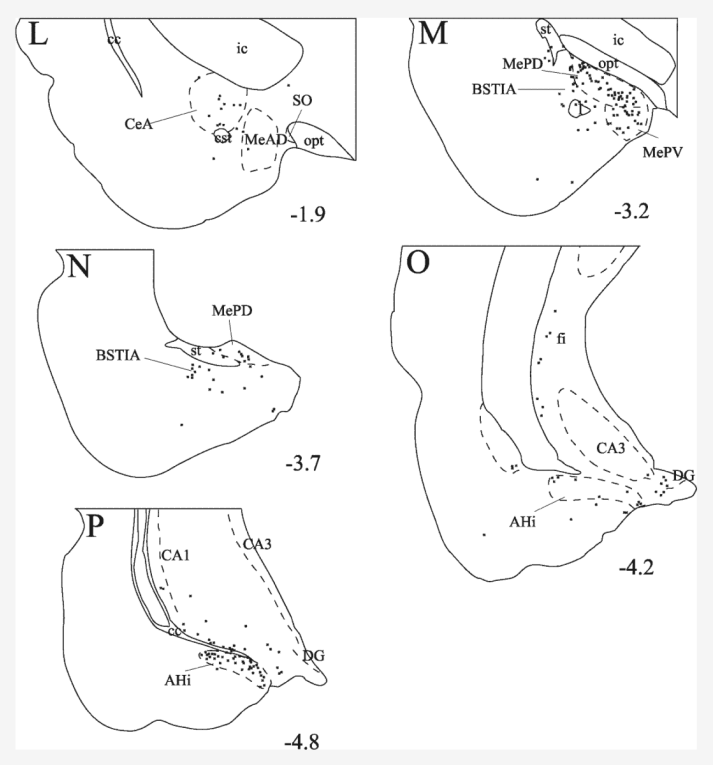

Fig. 3.

Schematic drawings of sections from case 117 illustrate the distribution of PHAL/proTRH-IR axons. Crosses represent double-labeled fiber segments. Numbers indicate the approximate distance of sections in mm from the Bregma. Regions of the amygdala and hippocampus are shown in images L-P.

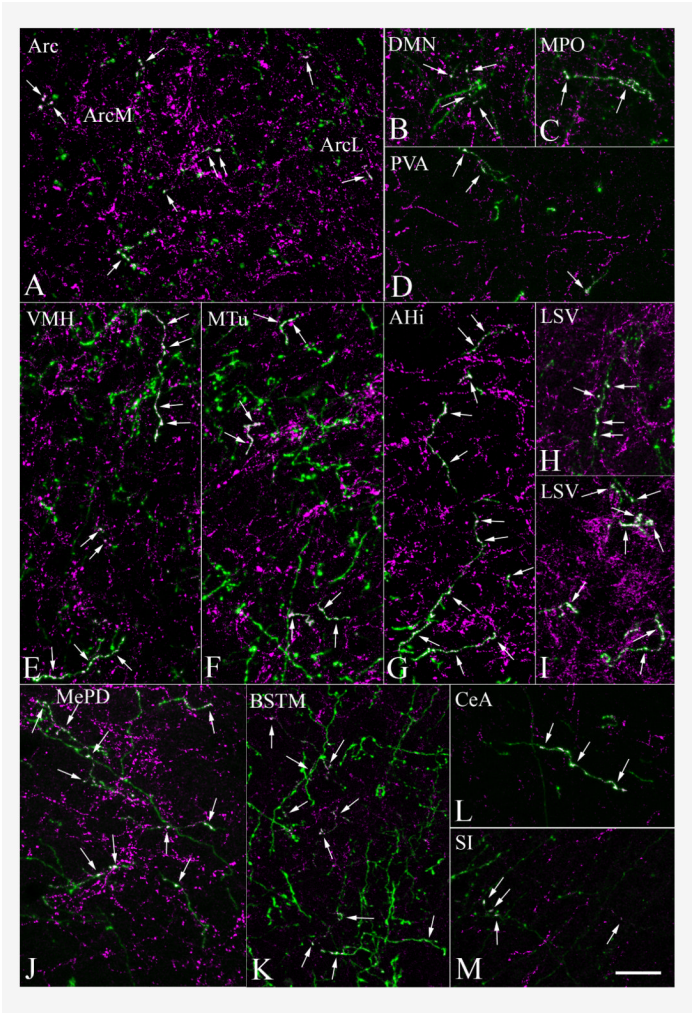

Fig. 4.

Double immunofluorescent staining demonstrates the presence of proTRH (magenta) in PHAL-containing (green) axons in different brain regions. Double-labeled axons (arrows) are indicated by the composite white color. Images represent five to twelve 1 μm thick confocal optical sections projected into one plane for better visualization of segments of double-labeled fibers. Images demonstrate PHAL/proTRH-containing fibers present in the (A) arcuate nucleus, (B) dorsomedial nucleus, (C) medial preoptic nucleus, (D) paraventricular thalamic nucleus, (E) ventromedial hypothalamic nucleus, (F) medial tuberal nucleus, (G) posteromedial part of amygdalohippocampal area, (H, I) lateral septal nucleus on the ipsilateral and contralateral sides, (J) posterodorsal part of the medial amygdaloid nucleus, (K) medial division of the bed nucleus of the stria terminalis, (L) central amygdaloid nucleus, (M) substantia innominata. Scale bar shown in (M) corresponds to 20 μm and refers to all micrographs.

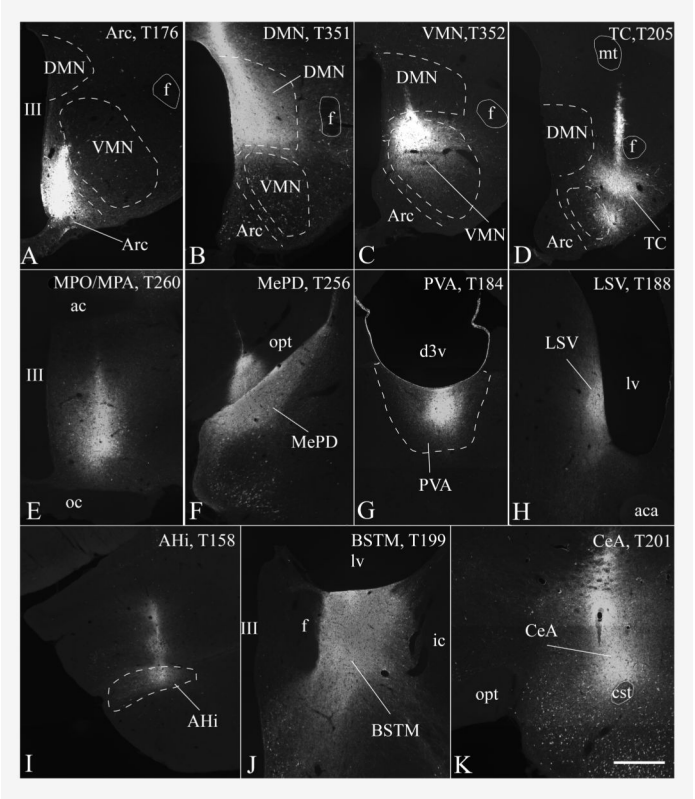

Fig. 5.

Cores of CTB injection sites centered in the (A) arcuate nucleus, (B) dorsomedial nucleus, (C) dorsomedial part of the ventromedial nucleus, (D) caudal part of the tuber cinereum area, (E) medial preoptic nucleus/medial preoptic area, (F) posterodorsal part of the medial amygdaloid nucleus, (G) paraventricular nucleus of the thalamus, (H) ventral part of the lateral septal nucleus, (I) amygdalohippocampal area, (J) posterior medial division of the BNST and (K) central amygdaloid nucleus. Case numbers are indicated in the images. Scale bar shown in (K) corresponds to 500 μm and refers to all micrographs.

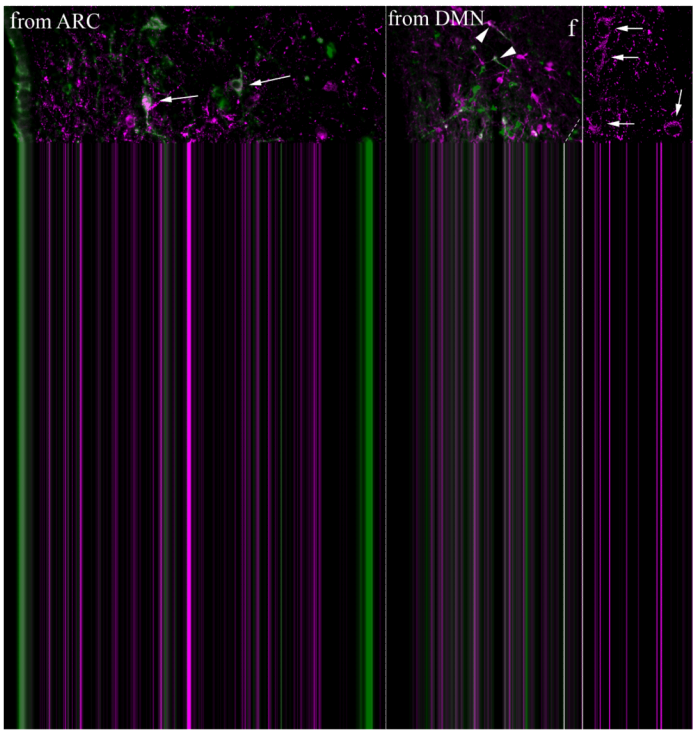

Fig. 6.

Double immunofluorescence demonstrates the presence of CTB (green) in TRH-IR (magenta) perikarya in the aPVN and perifornical area of brains previously injected with CTB into the (A) arcuate nucleus (ARC), (B) ventromedial nucleus (VMN), (C) dorsomedial nucleus (DMN), (D) medial preoptic nucleus/medial preoptic area (MPO/MPA) and (E) amygdalohippocampal area (AHi). Arrows point to CTB/TRH-IR neurons in the aPVN, arrowheads indicate CTB/TRH-IR neurons of the perifornical cell group. High magnification confocal images of single 1 μm thick optical sections were taken of framed areas in C and D, and are shown as insets. Inset of C shows TRH- and CTB-labeling in separate images to facilitate identification of double-labeled perikarya. Scale bar in B corresponds to 50 μm (for A and B), in D 100 μm (for C and D), in E 50 μm, and in the inset of D 10 μm (for inset images).

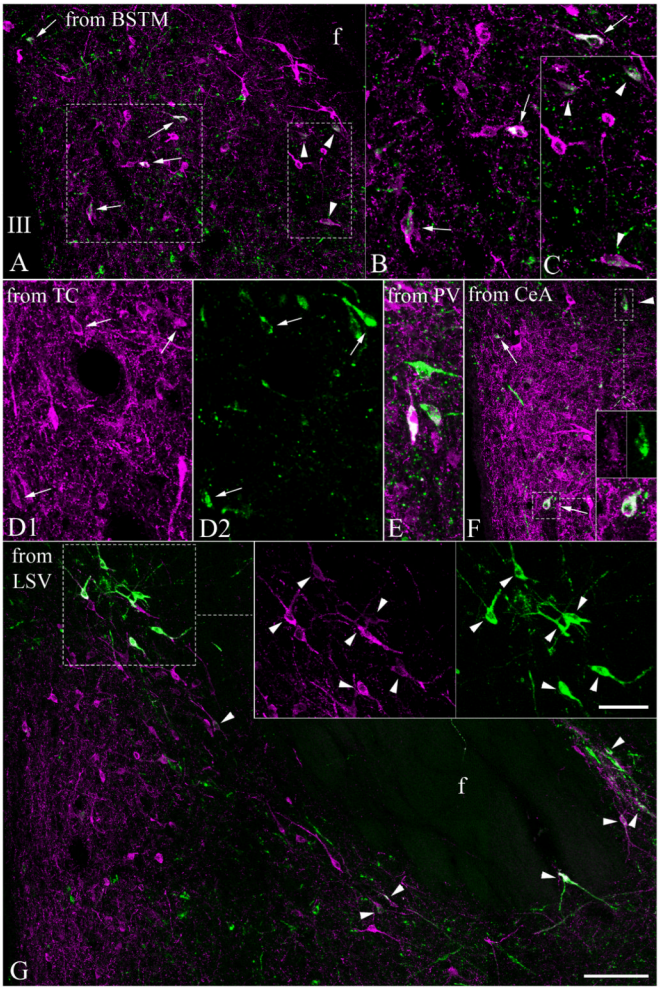

Fig. 7.

Double immunofluorescence demonstrates the presence of CTB (green) in TRH-IR (magenta) perikarya in the aPVN and perifornical area of brains previously injected with CTB into the (A-C) bed nucleus of the stria terminalis, posterior medial division (BSTM), (D1, D2) caudal part of the tuber cinereum area (TC), (E) paraventricular nucleus of the thalamus (PV), (F) central amygdaloid nucleus (CeA), (G) ventral part of the lateral septal nucleus (LSV). Images were made by projecting 4-7 consecutive 2 μm thick confocal optical slices into one plane. Arrows point to CTB/TRH-IR neurons in the aPVN, arrowheads indicate CTB/TRH-IR neurons of the perifornical cell group. Framed areas in A are magnified and shown in B and C, framed areas in F and G are magnified and shown in insets. To facilitate identification of double-labeled cells, TRH and CTB-labeling of the same fields are shown in separate images in D1 and D2, in the upper inset pair of F and in the inset of G. Scale bar shown in (F) corresponds to 100 μm in A, F, G, to 50 μm in B, C, D1, D2, E and insets of F. Scale bar in inset of G corresponds to 50 μm.

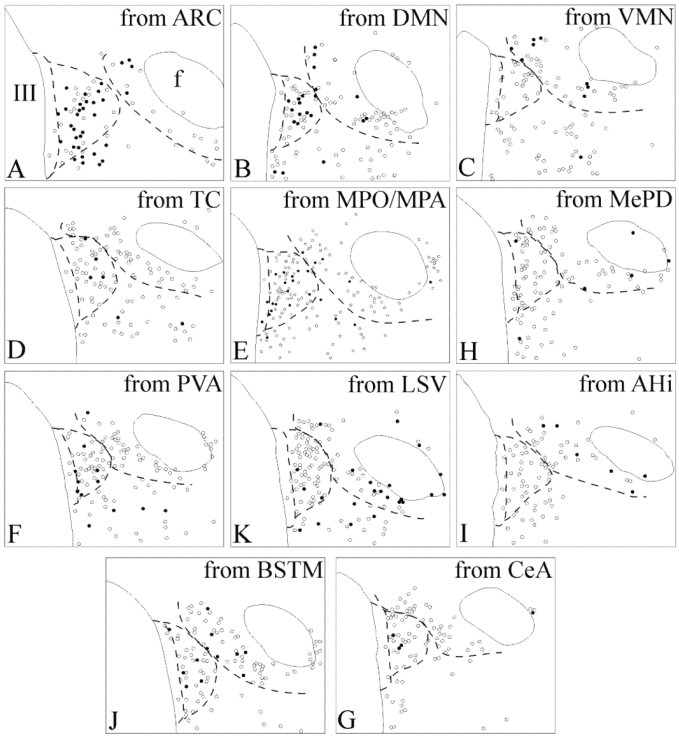

Fig. 8.

Schematic representation of retrogradely labeled TRH neurons in the aPVN and perifornical area following CTB injections into the (A) arcuate nucleus (ARC), (B) dorsomedial nucleus (DMN), (C) ventromedial nucleus (VMN), (D) caudal tuber cinereum area (TC), (E) medial preoptic nucleus/medial preoptic area (MPO/MPA), (F) medial amygdaloid nucleus (MePD), (G) paraventricular nucleus of the thalamus (PVA), (H) ventral part of the lateral septal nucleus (LSV), (I) amygdalohippocampal area (Hi), (J) bed nucleus of the stria terminalis, posterior medial division (BSTM) and (K) central amygdaloid nucleus (CeA). The corresponding injection sites are illustrated in Fig. 5. Open circles: single-labeled TRH neurons; solid circles: CTB/TRH double-labeled neurons. Dashed lines indicate the approximate borders of the periventricular parvocellular subdivision of the PVN, aPVN and the perifornical TRH cell group.

Table 1

Primary antibodies used

Antigen	Immunogen	Manufacturing	Dilution used
PHAL	purified PHAL	Vector Laboratories, rabbit polyclonal, # AS-2300	1:5,000
PHAL	purified PHAL	Vector Laboratories, goat polyclonal, AS-2224	1:1,000
proTRH178-199	synthetic peptide corresponding to rat preproTRH aa 178-199	Dr. Éva Rédei, rabbit polyclonal	1:2,500
CTB	purified CTB isolated from *Vibrio cholerae*	List Biological Labs, goat polyclonal, # 703	1:10,000
TRH	synthetic TRH	Dr. Ivor M. Jackson, rabbit polyclonal	1:2,500

Table 2

Evaluation of the density of PHAL/proTRH-IR fibers in cases 116 and 117

Regions	Density of PHAL/proTRH fibers
Hypothalamus and preoptic region	
Anterior hypothalamic area	**
Anterodorsal preoptic nucleus	***
Anteroventral periventricular nucleus	**
Arcuate nucleus	*****
Arcuate nucleus-ventromedial nucleus border	***
Dorsomedial nucleus	***
Dorsomedial nucleus-ventromedial nucleus border	****
Lateral hypothalamic area	**
Lateroanterior hypothalamic nucleus	*
Medial preoptic area	**
Medial preoptic nucleus	***
Medial tuberal nucleus	****
Paraventricular nucleus	*
Periventricular nucleus	**
Posterior hypothalamic area	*
Retrochiasmatic area	****
Strial part of the preoptic area	**
Suprachiasmatic nucleus	*
Supramammillary nucleus	*
Supraoptic nucleus	*
Tuber cinereum area	****
Ventral premammillary nucleus	***
Ventral tuberomammillary nucleus	*
Ventromedial nucleus	*****
Thalamus and epithalamus	
Lateral habenular nucleus	*
Mediodorsal thalamic nucleus	*
Paraventricular thalamic nucleus	***
Reuniens thalamic nucleus	*
Amygdala, hippocampus, substantia innominata	
Amygdalohippocampal area	*****
Anterior cortical amygdaloid nucleus	*
Basomedial amygdaloid nucleus	*
Bed nucleus of the stria terminalis, intraamygdaloid division	***
Central amygdaloid nucleus, capsular part	*
Central amygdaloid nucleus, medial division	***

Regions	Density of PHAL/proTRH fibers
Dentate gyrus	***
Ventral hippocampus, fields CA1 and CA3	***
Fimbria of the hippocampus	**
Lateral amygdaloid nucleus, ventromedial part	*
Medial amygdaloid nucleus, anterodorsal part	***
Medial amygdaloid nucleus, posterodorsal part	*****
Medial amygdaloid nucleus, posteroventral part	*****
Piriform cortex	*
Posterolateral cortical amygdaloid nucleus	*
Posteromedial cortical amygdaloid nucleus	*
Substantia innominata	***
Substantia innominata, basal part	**
Bed nucleus of the stria terminalis and septum	
Bed nucleus of the stria terminalis, lateral division	*
Bed nucleus of the stria terminalis, lateral division, dorsal part	*
Bed nucleus of the stria terminalis, lateral division, intermediate part	*
Bed nucleus of the stria terminalis, lateral division, ventral part	***
Bed nucleus of the stria terminalis, medial division, anterior part	*****
Bed nucleus of the stria terminalis, medial division, posterior part	*****
Bed nucleus of the stria terminalis, medial division, posterointermediate	****
Bed nucleus of the stria terminalis, medial division, posterolateral part	*****
Bed nucleus of the stria terminalis, medial division, ventral part	***
Lateral septal nucleus, dorsal part	*
Lateral septal nucleus, intermediate part	***
Lateral septal nucleus, ventral part	*****
Parastrial nucleus	*
Stria terminalis	**
Other telencephalic regions	
Anterior olfactory nucleus	*
Dorsal endopiriform nucleus	*
Islands of Calleja, major island	*
Medial septal nucleus	*
Nucleus of the horizontal limb of the diagonal band	*
Nucleus of the vertical limb of the diagonal band	*
Ventral pallidum	*
Zona limitans	**
Mesencephalon and hindbrain	

Regions	Density of PHAL/proTRH fibers
Lateral parabrachial nucleus, central part	*
Lateral periaqueductal gray	*
Periaqueductal gray	*
Ventral tegmental area	*
Ventrolateral periaqueductal gray	*

Table 3

Quantification of retrogradely labeled TRH neurons in the aPVN and perifornical area

Site of CTB injection	Case	Number of CTB/TRH-IR cells in the		
		aPVN[1]	perifornical area	
			in the level of the aPVN	caudal to the aPVN[2]
Arcuate nucleus, medial part	T176	45	5	0
Dorsomedial hypothalamic nucleus	T351	64	31	12
Ventromedial hypothalamic nucleus, dorsomedial part	T352	6	31	10
Ventromedial hypothalamic nucleus, ventromedial part	T177	4	22	3
Caudal part of the tuber cinereum area	T205	22	2	2
Ventral premammillary nucleus	T214	30	5	6
Medial preoptic nucleus / medial preoptic area	T260	43	31	5
Paraventricular thalamic nucleus	T183	15	1	1
Paraventricular thalamic nucleus	T184	25	2	2
Lateral septal nucleus, ventral part	T188	12	85	44
Lateral septal nucleus, ventral part / medial division of the BNST, anterior part	T197	28	60	18
Anterior and posterolateral part of the medial division of the BNST	T198	13	0	0
Medial division of the BNST, posterior part	T199	18	17	2
Central amygdaloid nucleus	T201	11	6	1
Medial amygdaloid nucleus, posterodorsal part	T256	6	10	2
Medial amygdaloid nucleus, posterodorsal part	T257	1	12	3
Medial amygdaloid nucleus, posteroventral part	T254	2	11	4
Amygdalohippocampal area	T155	1	11	5
Amygdalohippocampal area	T158	1	13	2

CTB/TRH neurons were counted in every fourth section on both the ipsilateral and contralateral sides

[1] included the CTB/TRH neurons in the periventricular parvocellular subdivision adjacent to the aPVN

[2] CTB/TRH neurons in the posterior part of the perifornical TRH cell group, located caudally to the antero-posterior level of the aPVN

Table 4

Major projection fields of TRH neurons in the aPVN and perifornical area identified by tract-tracing methods

aPVN TRH neurons	Perifornical TRH neurons
Arcuate nucleus	Ventromedial nucleus
Dorsomedial nucleus	Dorsomedial nucleus
Tuber cinereum area	Ventral premammillary nucleus
Ventral premammillary nucleus	Medial preoptic area and nucleus
Medial preoptic area and nucleus	Lateral septal nucleus
Paraventricular nucleus of the thalamus	Bed nucleus of the stria terminalis
Central amygdaloid nucleus	Medial amygdaloid nucleus
Bed nucleus of the stria terminalis	Amygdalohippocampal area
Lateral septal nucleus	